J. Fluid Mech. (1975), *vol.* 70, *part* 2, *pp.* 267–285
Printed in Great Britain

The propagation of planetary waves over a random topography

By RICHARD E. THOMSON

Environment Canada, Marine Sciences Directorate, Pacific Region,
1230 Government Street, Victoria, B.C.

(Received 5 January 1974 and in revised form 28 November 1974)

The purpose of this paper is to consider the effect of one-dimensional random depth variation on the propagation of planetary waves in a homogeneous layer of fluid having a free upper surface. We begin by determining the dispersion relation for the coherent part of the wave using the vorticity equation for the transport stream function and a previously described perturbation method. Then, from the resulting first-order expressions for the wavenumber, we obtain the phase speeds for the two possible planetary-wave solutions. These are compared with the corresponding phase speeds of planetary waves over a smoothly varying topography; the validity limits of the approximations are discussed. For the most physically realizable situation, of random depth correlation lengths much shorter than a typical wavelength, we find that the phase speed of the shorter (longer) wave component is less (greater) over a randomly varying topography than over a smoothly varying topography. In the case of the shorter waves, greatest relative changes in phase speed occur when the associated fluid motions are at right angles to the 'strike' of the roughness elements, while for both long and short waves there is no relative change in phase speed if fluid motions are parallel to the roughness contours. Moreover, both types of waves are shown to lose energy in the direction of energy propagation as a result of scattering. Numerical values are then obtained using hydrographic charts of the western North Pacific, and show that the randomness may significantly decrease the phase speed of the shorter planetary-wave component. Finally, we give a brief descriptive explanation of the results based on the effect of the topography on the wave restoring mechanism.

1. Introduction

Quasi-geostrophic waves play a major role in determining the planetary-scale circulations in the oceans. It is therefore essential to our understanding of large-scale motions to have detailed knowledge of the effects of bottom topography on the propagation of these waves.

In an incompressible fluid, planetary waves are governed dynamically by the conservation of potential vorticity following the motion, which requires any change in the absolute vorticity (relative plus planetary) of a column of fluid to be compensated for by an alteration in the length of its vortex lines. For the simplest case, of barotropic flow, the length of these lines is obtained directly

from the local fluid depth. The work of Rossby (1939) and Longuet-Higgins (1964, 1965) has shown the basic importance of the planetary vorticity tendency (the so-called β-effect) as a restoring mechanism for these waves, while Rhines (1969*a*, *b*) has demonstrated the greater importance of depth-induced vortex stretching as a restoring mechanism for the cases of a smoothly varying bottom and isolated topographic features. Rhines (1970) has also considered the linear resonant interaction (weak scattering) between two planetary waves in the presence of a "catalytic Fourier component" of the depth. More recently, Rhines & Bretherton (1973) have presented a fairly comprehensive study of the effects of 'rough' and 'smooth', sinusoidally varying topography on the propagation of planetary waves in a barotropic ocean having a rigid lid. Their results indicate that severe roughness of the topography reduces both the scale of the waves and their associated propagation of energy. Finally, a somewhat different problem has been considered by Keller & Veronis (1969), who determined the effect of random currents (effectively, a random background of relative vorticity advection) on the propagation of planetary waves.

In a sense, this paper is related to the latter two studies since we concern ourselves with the propagation of planetary waves over a rough bottom on which the topographic variations are considered to be a random variable. As in Keller & Veronis, our analysis is based on the method devised by Keller (1967) for finding the dispersion relation for an ensemble-averaged wave in a random medium. The criterion for the applicability of this method to the present problem is that $(\omega \sin\theta)^2 \epsilon^2 \Gamma(0)$ be somewhat less than unity, where ω is the Coriolis parameter divided by the wave frequency, θ is the angle of phase propagation relative to the depth gradient and $\epsilon^2\Gamma(0)$ is the mean-square fractional change in depth. For the ocean there will exist certain regions where the approximation fails for all possible waves, such as where seamounts (e.g. Cobb Seamount in the N.E. Pacific) penetrate close to the surface or where there exist islands or island arcs. Over many vast areas of the ocean, however, the results may be considered applicable.

In the next section, we present the appropriate vorticity equation for an ocean with a free surface having an exponentially varying mean depth upon which there is superimposed a random bottom fluctuation. The dispersion relation for the ensemble-averaged wave is then obtained following Keller (1967), and from this we derive expressions for the magnitudes of the two possible wavenumber components correct to second order in the fluctuations. In § 3, we use these expressions to show the effect of the random topography on the phase speed of planetary waves, and point out that the effect on the magnitude of the group velocity is qualitatively similar. Using topographic charts for the North Pacific published by Scripps University, we then obtain numerical values for the analytical expressions when the rough part of the topography has correlation lengths which are much shorter than typical wavelengths. Section 4 includes a discussion of the results and an attempt to explain physically what is taking place.

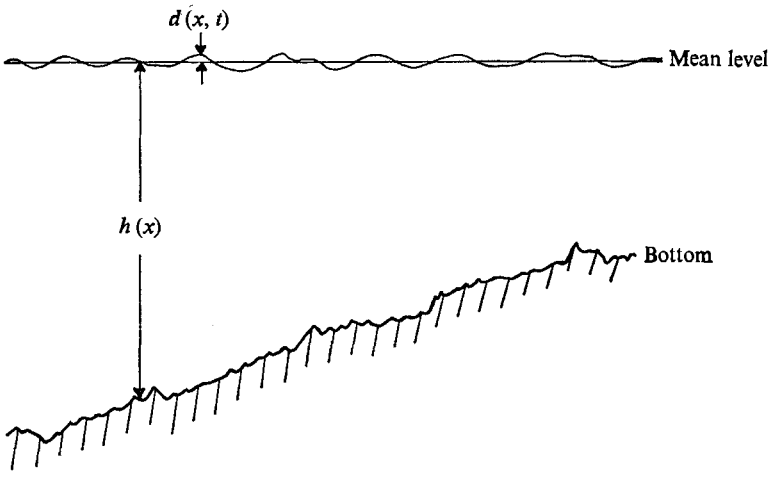

FIGURE 1. A vertical section through the fluid layer at right angles to the random depth variations. $h(\mathbf{x})$ is the time-averaged depth at $\mathbf{x}$ and $d(\mathbf{x}, t)$ is the time variation about this mean.

2. The dispersion relation

To derive the vorticity equation appropriate to a homogeneous incompressible fluid on a β-plane with a free upper surface, we follow the formulation of Thomson (1973). Somewhat similar derivations have also been presented by others (e.g. Rhines 1969*a*; Buchwald 1972).

Let (x, y, z) be the Cartesian co-ordinates in the eastward, northward and vertically upward directions, respectively, for a fluid having a total depth $H = d + h$ (figure 1), where $d(x, y, t)$ is the time-dependent surface elevation above the mean depth $h(x, y)$. By defining a scalar function ψ, associated with the non-divergent motions, and another scalar ϕ, associated with the surface divergent motions, through the relation

$$H\mathbf{u} = \boldsymbol{\kappa} \times \nabla\psi + \nabla\phi,$$

we find that the vertically integrated continuity equation can be written as

$$d_t + \nabla . (\nabla\phi) = 0. \tag{2.1}$$

Here, subscripts refer to partial differentiation, $\mathbf{u}$ is the velocity and $\boldsymbol{\kappa}$ is a unit vector in the $+z$ direction. Equation (2.1) may be combined with the vorticity equation derived from the linearized inviscid form of the momentum balance to yield an equation in ψ and ϕ. A second equation in these scalars is obtained by combining (2.1) with the divergence of the momentum balance. If we then assume that the radian frequency σ of the planetary waves is much less than the local inertial frequency f and also that the fractional changes in both the depth and f are $O(\sigma/f)$ over a wavelength, we obtain a simplified version of the vorticity equation; viz.

$$\nabla^2\psi_t + \beta\psi_x - \frac{1}{h}\left[f\nabla\psi \times \nabla h . \boldsymbol{\kappa} + \frac{f^2}{g}\psi_t\right] = 0, \tag{2.2}$$

in which ∇^2 is the two-dimensional Laplacian operator and $\mathbf{g}$ is the acceleration due to gravity. In deriving (2.2), we have further assumed that $d \ll h$ and that $f = f_0 + \beta y$ (f_0 and β being constants) when it appears differentiated with respect to y (the β-plane approximation).

For a locally constant f and sinusoidal motions, (2.2) gives the energetically correct relation of a purely real wave frequency for real wavenumbers, whereas the more general vorticity equation does not. In the latter case, Veronis (1966) has shown that it is necessary to allow for spatial variations in both f and the stream-function magnitude to obtain such a relation. Moreover, since we shall be considering h to have a random variation about a mean value, the exact wave field ψ will be a random function. This exact solution must then be written as $\psi = \langle\psi\rangle + \psi'$, where the angular brackets represent an ensemble average over many realizations of the flow field in a particular topographic region, with ψ' representing deviations of the exact wave from the coherent or mean field $\langle\psi\rangle$ over that region. (Such realizations must be thought of as initiated by the same process with the space-time values in the region taken at the same phase.) If the spatial amplitude of ψ were modulated by the depth, as is necessary in Veronis' case, it would not be possible to obtain a simple relationship for $\langle\psi\rangle$ since averages of the product of the random part of the depth and the random part of the stream function would need to be included. In the analysis of (2.2) however, these complications do not arise and the physics of the situation can be understood by consideration of the coherent wave alone.

The problem now involves specifying a realistic model for the depth. If one looks at recent bathymetric charts of the ocean, such as those produced by Chase, Menard & Mammerickx (1970) for the North Pacific, it is clear that the most general description of the topography would involve a gently sloping mean depth upon which are superimposed abrupt features such as seamounts, ridges and trenches. The latter two, of course, have a definite orientation, with depth variations along the strike being relatively small compared with depth variations at right angles to this direction. However, depths in the normal direction appear to be randomly distributed. The seamount distributions within a given locality do not in general have a preferred direction, although the mean slope upon which they are superimposed does. None the less, there are regions of seamount chains which show a greater and more random variation in depth along one direction than along the other. In order to obtain relatively straightforward analytical results, we therefore limit our discussion to oceanic regions exhibiting such preferred depth orientations. Furthermore, we assume, for the sake of simplicity, that any trend in the mean depth profile varies exponentially with distance. Any other type of modelling of the mean depth would detract from the usefulness of the results by greatly complicating the problem.

Suppose that the co-ordinate in the preferred direction of depth variation about the mean is ξ, and that depth changes about the mean in the η direction, at right angles to this, are significantly smaller. Then the transformation to co-ordinates orientated along these fluctuating depth variations is

$$\begin{pmatrix} \xi \\ \eta \end{pmatrix} = \begin{pmatrix} \cos\alpha & \sin\alpha \\ -\sin\alpha & \cos\alpha \end{pmatrix} \begin{pmatrix} x \\ y \end{pmatrix},$$

where $-\frac{1}{2}\pi < \alpha < \frac{1}{2}\pi$ in order to avoid any ambiguity in the definition of orientation. If we now assume that the stream function has the separable time dependence

$$\psi(\xi, \eta, t) = \exp(-i\sigma t)\,\Psi(\xi, \eta),$$

with $\sigma > 0$ and real, and that the depth has the form

$$h(\xi, \eta) = h_0 \exp(m\xi + n\eta)\,[1 + \epsilon\mu(\xi)],$$

where h_0, m and n are constants, $0 < \epsilon \ll 1$ and μ is a zero-mean random variable, we may write (2.2) to $O(\epsilon)$ as

$$\left[\nabla^2 - \gamma_0^2 + \frac{i}{\sigma}(\beta\cos\alpha - f_0 n)\frac{\partial}{\partial\xi} - \frac{i}{\sigma}(\beta\sin\alpha - f_0 m)\frac{\partial}{\partial\eta}\right]\Psi + \epsilon\left[i\frac{f_0}{\sigma}\frac{\partial\mu}{\partial\xi}\frac{\partial}{\partial\eta}\right]\Psi = 0. \tag{2.3}$$

In deriving (2.3), we have made the additional assumptions that $f \simeq f_0$ and $(f^2/gh)\exp[-(m\xi + n\eta)] \simeq f_0^2/gh_0 = \gamma_0^2$. For the former assumption to be valid, we require that f changes little over a wave scale; i.e. that

$$\lambda_y \ll 2\pi f_0/\beta,$$

where λ_y is the wavelength in the northern direction. Clearly, the approximation fails near the equator for much shorter wavelengths than at mid-latitudes. At 5° latitude, for example, $\lambda_y \ll 3000$ km while at 40° this limit rises to 30000 km. The requirement that $m\xi + n\eta \ll 1$ in the surface divergent term implies that changes in the mean depth are small over a wave scale. Since $|m|, |n| \simeq \bar{h}^{-1}|\nabla\bar{h}|$, where $\bar{h}$ is the mean depth, this requires that $\Delta\bar{h}/\bar{h} \ll 1$ over a wavelength, which is the basic assumption in our derivation of (2.2). We note here that the surface divergence is included in the deterministic part of (2.3) simply to allow for the existence of two planetary-wave solutions for a given frequency. At worst, surface divergence contributes a term of order $\epsilon^2\gamma_0^2\lambda^2$ (where $\gamma_0^2\lambda^2 \ll 1$) to the random operator, and this is small in comparison with the $O(\epsilon^2)$ contribution from depth variations.

Equation (2.3) has the form

$$(L + M)\,\Psi = 0,$$

where
$$L = \nabla^2 - \gamma_0^2 + \frac{i}{\sigma}\left[(\beta\cos\alpha - f_0 n)\frac{\partial}{\partial\xi} - (\beta\sin\alpha - f_0 m)\frac{\partial}{\partial\eta}\right] \tag{2.4}$$

is a linear deterministic differential operator and

$$M = \epsilon\left(i\frac{f_0}{\sigma}\frac{\partial\mu}{\partial\xi}\frac{\partial}{\partial\eta}\right) \tag{2.5}$$

is a linear centred (i.e. zero-mean) random differential operator. When M is a small perturbation of the deterministic operator L, in the sense that the norm $\|L^{-1}M\|$ is less than unity, we may obtain the dispersion relation for the ensemble-averaged stream function $\langle\psi(\xi, \eta, t)\rangle$ using the method described by Keller (1967). In particular, we find that the first-order approximation to the dispersion relation is

$$\exp[-i(k\xi + l\eta)]\,[L - \langle ML^{-1}M\rangle]\exp[+i(k\xi + l\eta)] = 0, \tag{2.6}$$

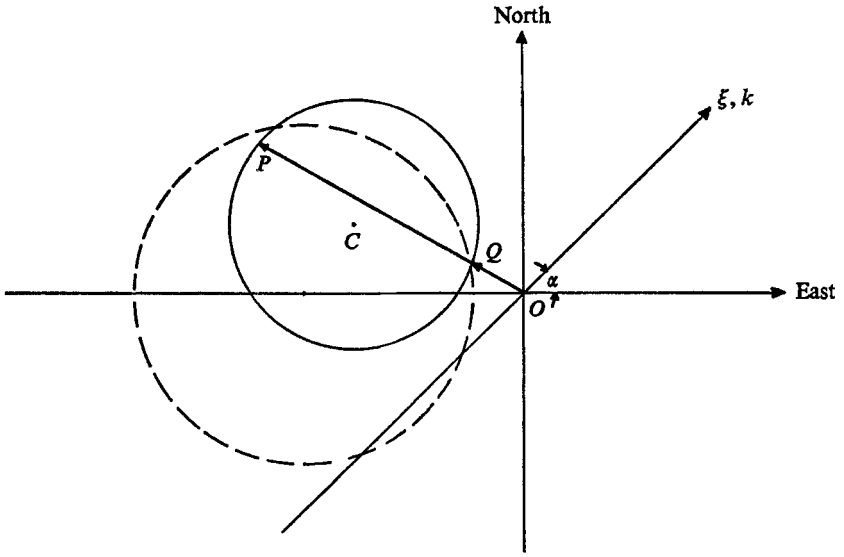

FIGURE 2. A plot of the slowness curves (σ = constant) for planetary waves in a layer of fluid having a uniform mean depth (dashed circle) and in a fluid layer having a mean depth decreasing to the east (solid circle). The variables ξ and k are, respectively, the position co-ordinate and wavenumber component across the random depth variations, which are orientated at an angle α to east. OP and OQ are in the directions of the short and long wave components, respectively. C is the centre of the solid circle.

which for $M \equiv 0$ yields the deterministic relation for planetary waves

$$\sigma(k,l) = -\frac{k(\beta\cos\alpha - f_0 n) - l(\beta\sin\alpha - f_0 m)}{k^2+l^2+\gamma_0^2}. \tag{2.7}$$

Setting $m = n = 0$ in (2.7) results in the usual dispersion relation for Rossby waves (h uniform). A plot of the 'slowness curves' (the curves σ = constant in wavenumber space) for the cases of a uniform and a slowly varying mean depth is presented in figure 2. In each case, there are (for a given frequency and direction of phase propagation) two waves, one short and one long, corresponding to where the circle cuts a line drawn from the origin. Clearly, the effect of the topography is to 'swing' the locus of possible wavenumbers about the origin by adding to the Rossby wavenumbers a topographic component which always moves with deep water to its left in the northern hemisphere. The short waves in this case, then, have their phase propagation in the direction OP, long-wave phase propagation being in the direction OQ. The group velocities are in the directions PC and QC, respectively.

We now wish to determine the correction to the wavenumbers in (2.7) brought about by the ensemble average of the random operator in (2.6). To do this we need to know the form of the operator L^{-1}. Let us, then, define

$$L^{-1}q(\xi,\eta) = \iint_{-\infty}^{\infty} G(\xi-\xi',\eta-\eta')\,q(\xi',\eta')\,d\xi'\,d\eta', \tag{2.8}$$

where G is the Green's function,

$$LG(\xi,\eta) = \delta(\xi)\,\delta(\eta), \tag{2.9}$$

and δ is the Dirac delta function. A double Fourier transform of (2.9) then produces $\hat{\hat{G}}(k,l)$, which, when inverted with respect to k, yields the single transform in η, $\hat{G}(\xi,l)$.

As the poles associated with the latter transform lie on the real k axis, the path of integration in the complex k plane must be indented around them in such a way that the transformed Green's function $\hat{G}(\xi,l)$ produces outward-propagating energy along ξ, in accordance with the Sommerfeld radiation condition. The analysis therefore involves determination of the components of the group velocity along ξ for the two possible waves. For

$$B = -(2\sigma)^{-1}(\beta\cos\alpha - f_0 n)$$

and

$$D = 1 - B^{-2}[l^2 + \gamma_0^2 - (l/\sigma)(\beta\sin\alpha - f_0 m)],$$

the result is found to be

$$\hat{G}(\xi,l) = (i/2|B|D^{\frac{1}{2}})\exp[i(B\xi - D^{\frac{1}{2}}|B||\xi|)], \tag{2.10}$$

which may now be applied to the analysis of the correction term through use of (2.8).

Application of (2.5) and (2.8) to the exponential in (2.6) gives

$$L^{-1}M\exp[i(k\xi+l\eta)] = -\epsilon\iint_{-\infty}^{\infty} G(\xi-\xi',\eta-\eta')\left(l\frac{f_0}{\sigma}\frac{\partial\mu}{\partial\xi'}\right)\exp[i(k\xi'+l\eta')]\,d\xi'\,d\eta'.$$

If we now transform this equation via the new variables $\xi - \xi' = \hat{\xi}$ and $\eta - \eta' = \hat{\eta}$ and use the relation $\partial\mu/\partial\xi' = -\partial\mu/\partial\hat{\xi}$, we find that

$$L^{-1}M\exp[i(k\xi+l\eta)] = \epsilon\exp[i(k\xi+l\eta)]\int_{-\infty}^{\infty}\hat{G}(\hat{\xi},l)\,e^{-ik\hat{\xi}}\left(l\frac{f_0}{\sigma}\frac{\partial\mu}{\partial\hat{\xi}}\right)d\hat{\xi}, \tag{2.11}$$

in which we have also taken the opportunity to invert one integral with respect to η. Use of (2.5) on (2.11) and ensemble averaging finally yields

$$\langle ML^{-1}M\rangle\exp[i(k\xi+l\eta)] = \epsilon^2\exp[i(k\xi+l\eta)]\int_{-\infty}^{\infty}\hat{G}(\hat{\xi},l)\,e^{-ik\hat{\xi}}S(\hat{\xi})\,d\hat{\xi}, \tag{2.12}$$

in which

$$S(\hat{\xi}) = -\left(l\frac{f_0}{\sigma}\right)^2\frac{d^2\Gamma(\hat{\xi})}{d\hat{\xi}^2} \tag{2.13}$$

is defined in terms of

$$\Gamma(\hat{\xi}) = \langle\mu(\xi)\mu(\xi-\hat{\xi})\rangle, \tag{2.14}$$

the autocovariance function for the depth fluctuations. The dispersion relation (2.6) for the coherent waves is then obtained using (2.4) and (2.12). To $O(\epsilon^2)$, the result is

$$K^2 + K\left[\frac{\beta}{\sigma}\cos(\theta+\alpha) + \frac{f_0}{\sigma}(m\sin\theta - n\cos\theta)\right] + \gamma_0^2 + \epsilon^2\int_{-\infty}^{\infty}\hat{G}(\hat{\xi},l)\,e^{-ik\hat{\xi}}S(\hat{\xi})\,d\hat{\xi} = 0, \tag{2.15}$$

where we have transformed the deterministic part of this relation via the polar co-ordinates

$$(k,l) = K(\cos\theta,\sin\theta). \tag{2.16}$$

As a consequence of (2.16), we may consider (2.15) as an equation for K as a function of σ and θ with the parameters f_0, β and α. Solutions to (2.15) are found

through an iteration procedure, in which the zeroth-order approximations are obtained by setting $\epsilon = 0$. The first-order smoothing or iterative solutions are then found by substituting the respective zeroth-order solutions into the ϵ^2-term. Therefore, letting

$$\mathbf{K}_{j0} = (k_{j0}, l_{j0}) \quad (j = 1, 2) \tag{2.17}$$

define the wavenumber components for the two zeroth-order solutions of (2.15) and using expression (2.10) for $\hat{G}(\xi, l_{j0})$, we obtain to $O(\epsilon^2)$

$$K^2 + K\beta^*/\sigma + \gamma_0^2 + \epsilon^2 \left\{ [2(k_{j0} - B)]^{-1} \int_0^\infty \sin[2(k_{j0} - B)\,\xi]\, S(\xi)\, d\xi \right.$$
$$\left. + i\,|k_{j0} - B|^{-1} \int_0^\infty \cos^2[(k_{j0} - B)\,\xi]\, S(\xi)\, d\xi \right\} = 0, \tag{2.18}$$

in which

$$\beta^* = \beta\cos(\theta + \alpha) + f_0(m\sin\theta - n\cos\theta) \tag{2.19}$$

is a modified β-effect and where we have used the fact that $\Gamma(\xi)$ is an even function and that $D^{\frac{1}{2}} = |k_{j0} - B|/|B|$, to the order required.

Integrating by parts in (2.18) after substitution of (2.13), we finally obtain

$$K^2 + K\beta^*/\sigma + \gamma_0^2$$
$$- \epsilon^2 \left\{ \left(l_{j0} \frac{f_0}{\sigma} \right)^2 \left[\Gamma(0) - 2i\,|k_{j0} - B| \int_0^\infty \Gamma(\xi) \exp[-2i\,|k_{j0} - B|\,\xi]\, d\xi \right] \right\} = 0, \tag{2.20}$$

in which we have used the fact that $d\Gamma(0)/d\xi = 0$ for any autocovariance function.

Letting $\epsilon^2 R$ be defined by the last expression in (2.20), we may solve for the two roots K_j $(j = 1, 2)$:

$$K_j = -\frac{1}{2}\frac{\beta^*}{\sigma} - (-1)^j \left\{ \left(\frac{1}{2}\frac{\beta^*}{\sigma} \right)^2 - \gamma_0^2 \right\}^{\frac{1}{2}} \left\{ 1 - \left[\left(\frac{1}{2}\frac{\beta^*}{\sigma} \right)^2 - \gamma_0^2 \right]^{-1} \epsilon^2 R_j \right\}^{\frac{1}{2}}, \tag{2.21}$$

where R_j is the value of R for the wavenumber of the zeroth-order solution ($\epsilon = 0$)

$$K_{j0} = -\tfrac{1}{2}\beta^*/\sigma - (-1)^j \{(\tfrac{1}{2}\beta^*/\sigma)^2 - \gamma_0^2\}^{\frac{1}{2}}. \tag{2.22}$$

Since the K's must be positive-definite quantities, the angle θ in (2.19) must be chosen such that $\beta^* < 0$. For Rossby waves ($m = n = 0$) this limits the direction of phase propagation to

$$\tfrac{1}{2}\pi - \alpha < \theta < \tfrac{3}{2}\pi - \alpha,$$

while for waves in a fluid of variable mean depth the range of θ will depend upon the magnitude and sign of the parameters m and n.

The validity of the first-order smoothing is seen from (2.21) to require that the magnitude of the correction term $\epsilon^2 R_j$ be somewhat less than the zeroth-order term $(\frac{1}{2}\beta^*/\sigma)^2 - \gamma_0^2$. Moreover, the surface divergent effect must always be smaller than the combined effects of the latitudinal variation of the Coriolis parameter and the depth gradient (i.e. $\gamma_0 < \frac{1}{2}\beta^*/\sigma$) in order that real solutions to (2.22) are obtained. Therefore, if we assume that we can ignore higher-order terms in an expansion in $\gamma_0(\frac{1}{2}\beta^*/\sigma)^{-1}$, the two zeroth-order solutions from (2.22) are to a good approximation

$$K_{10} = -\beta^*/\sigma + \gamma_0^2\sigma/\beta^*, \quad K_{20} = -\gamma_0^2\sigma/\beta^*,$$

which together with (2.16) and (2.17) permit us to determine R_1 and R_2, and therefore the first-order wavenumbers (2.21). These are to $O(\epsilon^2)$

$$K_1 = K_{10} - \epsilon^2 (K_{10} - K_{20})^{-1} R_1 \tag{2.23}$$

and

$$K_2 = K_{20} + \epsilon^2 (K_{10} - K_{20})^{-1} R_2, \tag{2.24}$$

where $K_{10} - K_{20} > 0$ and where the R's are given by the ϵ^2-term in (2.20). In expanded form these complex quantities are

$$R_j = -\left(l_{j0}\frac{f_0}{\sigma}\right)^2 \Gamma(0) + \left(l_{j0}\frac{f_0}{\sigma}\right)^2 \left\{2(k_{j0} - B)\int_0^\infty \Gamma(\hat{\xi}) \sin\left[2(k_{j0} - B)\,\hat{\xi}\right] d\hat{\xi} + i2|k_{j0} - B| \int_0^\infty \Gamma(\hat{\xi}) \cos\left[2(k_{j0} - B)\,\hat{\xi}\right] d\hat{\xi}\right\} \tag{2.25}$$

for $j = 1, 2$. In (2.25), $\Gamma(0)$ measures the mean square of the depth fluctuations while the integrals represent an interaction between the waves and the topography.

3. Wave amplitude and phase speed

The real parts of relationships (2.23) and (2.24) can now be used to find the ratios of both the phase speeds and group-velocity magnitudes of the waves in a surface divergent fluid of smoothly varying depth to those in a fluid with a superimposed random depth variation. (Although we shall confine our attention to the analytically simpler phase-speed expression, it should be noted that the results for the group-velocity components are qualitatively similar since they too are proportional to the magnitude of the wavenumber.) The change in amplitude of the ensemble-averaged stream function due to scattering is obtainable from the imaginary parts of these relationships. Letting

$$C_{j0} = \sigma / K_{j0}$$

be the phase speeds in the absence of bottom roughness and

$$C_j = \sigma / \mathrm{Re}\{K_j\} \tag{3.1}$$

those when there is rough topography, we find from (2.23)–(2.25) that

$$C_{j0}/C_j - 1 = (-1)^j \epsilon^2 \,\mathrm{Re}\{R_j\} / K_{j0}(K_{10} - K_{20}) \tag{3.2}$$

for $j = 1, 2$. The validity of the first-order smoothing is now dependent upon the magnitude of the right-hand side of (3.2) being much less than unity. Thus, for a given region having a particular configuration of topographic roughness, there will be a finite range of wavenumbers for which the results are applicable. The greater the mean-square depth the more limited this range, as one would expect for a problem including a first-order smoothing technique.

When the right-hand side of (3.2) is negative, the planetary waves over the irregularly varying bottom have a larger phase speed than those over a smoothly varying bottom while a positive value indicates the reverse situation. Using (2.25), therefore, it is clear that the effect of the mean-square depth range $\Gamma(0)$ is

to decrease the phase speed of the short wave component and to increase the phase speed of the long wave component. On the other hand, the effect of the integral term can be to decrease or increase the wave speed of the two components. In either case, there is no change in phase speed if the actual fluid motions are parallel to the roughness contours (i.e. $l_{j0} = 0$).

The imaginary parts of the K_j, which determine the change in amplitude of the two solutions $\langle \psi_j \rangle$ in the direction of phase propagation, are found from (2.25) to be

$$\mathrm{Im}\{K_j\} = (-1)^j \epsilon^2 (K_{10} - K_{20})^{-1} \left\{ 2\pi \left(\frac{l_{j0} f_0}{\sigma} \right)^2 |k_{j0} - B| \, E[2(k_{j0} - B)] \right\}, \quad (3.3)$$

in which the bracketed term is $\mathrm{Im}\{R_j\}$ and where

$$E[2(k_{j0} - B)] = \frac{1}{2\pi} \int_{-\infty}^{\infty} \Gamma(\hat{\xi}) \exp[2i(k_{j0} - B)\hat{\xi}] \, d\hat{\xi} \quad (3.4)$$

represents an energy spectrum for the interaction of the planetary waves with the bottom topography. Since the bracketed terms in (3.3) are non-negative, we find $\mathrm{Im}\{K_1\} < 0$ for the short wave component and $\mathrm{Im}\{K_2\} > 0$ for the long wave component, which signifies that in the direction of phase propagation the magnitude of $\langle \psi_1 \rangle$ is increasing while that of $\langle \psi_2 \rangle$ is decreasing. However, as the sign of the group-velocity component across the roughness contours is opposite to that of the corresponding phase-velocity component for the short waves and the same for the long waves, there is always a decrease in the amplitude of the ensemble-averaged stream function in the direction of energy propagation. The only exceptions are when the actual fluid displacements and the direction of amplitude modulation (i.e. the group-velocity direction) are parallel to the roughness contours ($l_{j0} = 0$ and $k_{j0} - B = 0$, respectively). In these cases there is no amplitude change in the direction of phase propagation.

The expression for R_j may be simplified by considering the two asymptotic limits $L/\lambda \ll 1$ and $L/\lambda \gg 1$, where L is the correlation length for the depth variations and λ is the characteristic wavelength. The correlation length is the distance beyond which the correlation between depths becomes negligible, i.e. $\Gamma(\xi) \simeq 0$ for $|\xi| > L$.

Short correlation lengths

Suppose that the wavelength of the planetary waves is much greater than the distance over which the bottom features are correlated. Then, substituting $2(k_{j0} - B) = 4\pi/\lambda$ and $\xi = L\xi'$ into (2.25), we find upon retaining only the first terms in the expansion in L/λ that

$$\mathrm{Re}\{R_j\} = -(l_{j0} f_0/\sigma)^2 \Gamma(0) \quad (3.5)$$

and

$$\mathrm{Im}\{R_j\} = (l_{j0} f_0/\sigma)^2 E'(0) \, O(L/\lambda), \quad (3.6)$$

where

$$E('0) = \frac{1}{2\pi} \int_{-1}^{+1} \Gamma(L\xi') \, d\xi'$$

and in which we have assumed that the integrals

$$\int_{-\infty}^{\infty} \Gamma(L\xi') \, \xi'^p \, d\xi' \sim \int_{-1}^{+1} \Gamma(L\xi') \, \xi'^p \, d\xi', \quad p = 0, 1, 2, \ldots,$$

are of order unity.

The phase-speed relation (3.2) thereby reduces to the simple form

$$C_{j0}/C_j - 1 = (-1)^{j+1}\epsilon^2 \frac{K_{j0}(f_0\sigma^{-1}\sin\theta)^2\,\Gamma(0)}{K_{10}-K_{20}}, \tag{3.7}$$

so that the relative change in phase speed is strictly dependent upon the mean square of the depth fluctuations about the mean profile. In this limit, then, the short planetary-wave component has a slower phase speed than a wave of the same frequency propagating over a smoothly varying depth. The long wave component, on the contrary, has a greater phase speed with the relative change being less than that for the short wave by the ratio K_{20}/K_{10}, all other factors being equal.

As indicated by $\mathrm{Im}\{R_j\}$ in (3.6), the effect of the random bottom on the amplitude of the mean stress functions is very small for short correlation lengths, and is typical of situations in which the dimension of the scatterers is much less than that of the waves.

Although the short-correlation limit is much more applicable to the real ocean than the long-correlation limit, as we shall show presently, the latter is included here for the sake of completeness.

Long correlation lengths

In this case we consider the limit $L/\lambda \gg 1$. Since this necessitates $k_{j0} - B \neq 0$, the range of validity of this approximation is much more restrictive than that for the limit of short correlation lengths. Moreover, the fact that the argument of the circular functions in (2.25) is large implies that the integrals will be small. To obtain an asymptotic expansion in λ/L, therefore, we need to integrate by parts, from which it follows that both $\mathrm{Re}\{R_j\}$ and $\mathrm{Im}\{R_j\}$ are at most of order $(\lambda/L)^2$. In this limit, then, neither the phase speed nor the amplitude of the waves is much affected by the random topography.

A numerical example

In order to give quantitative values to the phase speeds derived previously, we use a series of bathymetry charts for the North Pacific published by Scripps University (Chase *et al.* 1970). From these charts it can be seen that the extensive region west of North America extending to about 160° W longitude and south of 50° N latitude appears to be reasonably well suited to our model. In particular, the mean depth in the northern direction remains nearly uniform at about 5000 m while the orientations of the major fracture zones which cross the region remain consistently east–west. Figure 3 shows two typical north–south profiles of $\epsilon\mu$. The predominent features, having longitudinal extent exceeding 40°, are the Clipperton and Molokai fracture zones between 5–7° N and 23–26° N latitude, respectively, and the more rugged Clarion and Murray fracture zones between 14–17° N and 30–33° N latitude, respectively. The more northerly situated Mendocino fracture zone has not been included in the examples although its east–west strike continues the pattern established by the fracture zones to the south. The large peak at about 23° N on the 127° W longitude line in figure 3

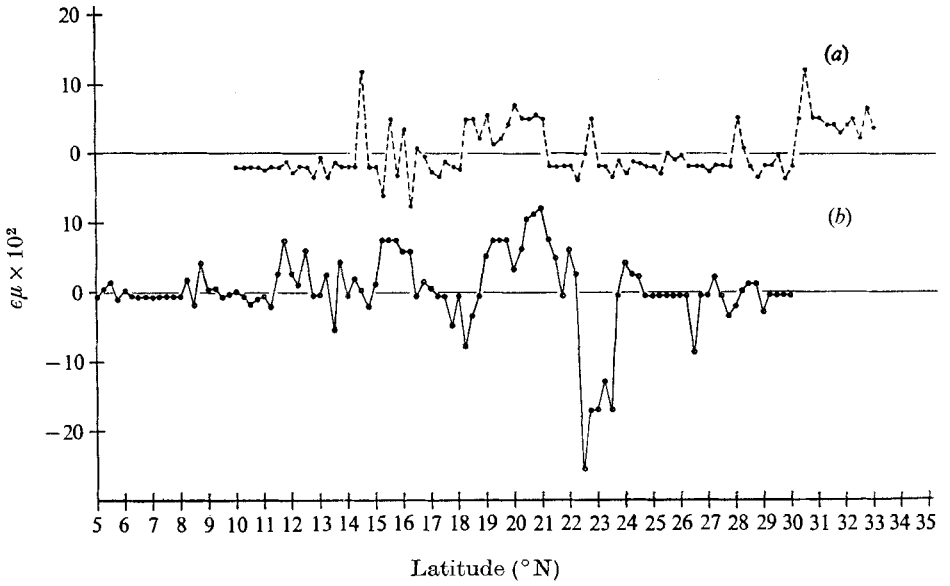

FIGURE 3. Normalized variations in depth as a function of latitude y for two meridians of longitude (*a*) 145° W and (*b*) 127° W in the western North Pacific. The mean depth in the northern direction is assumed uniform (h_0), so that $\epsilon\mu(y) = h(y)/h_0 - 1$. Depths have been interpolated from topographic charts of the North Pacific published by the University of California, La Jolla (Chase *et al.* 1970).

marks the location of one of the isolated seamounts that occur within the region. Since $\epsilon\mu < O(10^{-1})$, it is clear that the topography in this extensive region satisfies the assumption concerning the smallness of the random variations. Also, the fractional eastward decrease in the east–west profile of the mean depth is at most 40 % from 160° W longitude to 115° W longitude and appears to approximate the exponential behaviour specified in the model.

In connexion with the above depths, it should be mentioned that the values assigned between plotted contours on the charts are not based on actual soundings. Rather, they are based on a random selection of the depth every 15′ according to the maximum amount of relief possible in a given area as indicated schematically on the charts. The relative change in depth beginning with a specified contour is then chosen as a fraction of this maximum value by rolling a pair of dice. A total of 7 represents zero change (i.e. 0/5) while 12 and 2 represent positive and negative fractional changes of 5/5, respectively, the normal distribution curve for a pair of dice tending to weight smaller depth increments.

The autocovariances obtained from the depth variations are plotted in figure 4 for lag increments of 15′ latitude. They appear to support the assumption of a random topography at Rossby-wave scales (> 10 km) since in both examples the normalized autocovariances are less than 0·5 after lags of only 15′ ($\sim$ 25 km). Of course, depth changes on scales less than 25 km, which will undoubtedly affect the propagation of barotropic planetary waves, are absent from these calculations because of the limited accuracy of the bathymetric charts used. Moreover, the analysis used in this paper, being based strictly on the conservation of potential

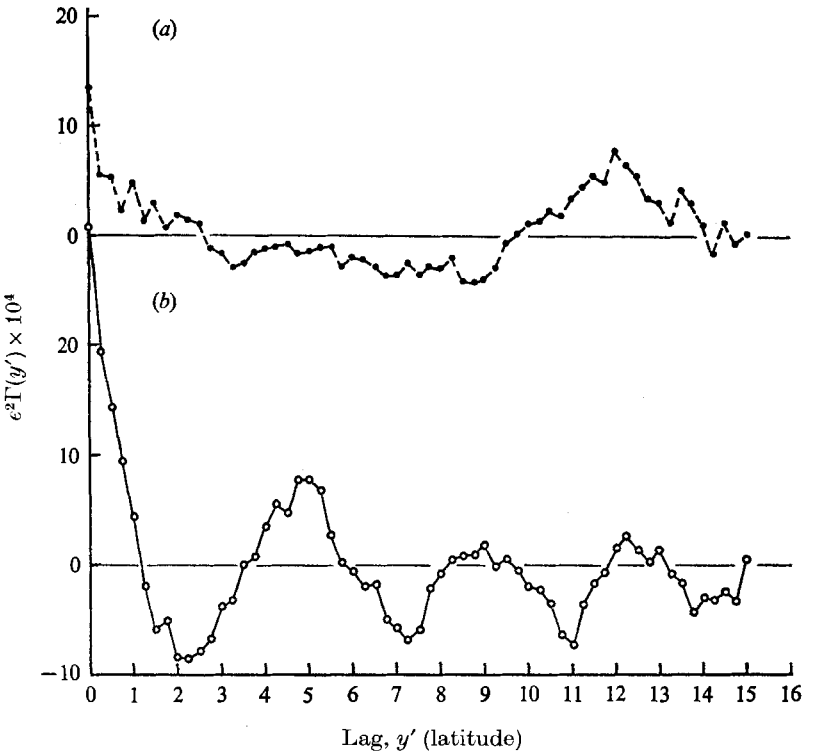

FIGURE 4. The autocovariance $\Gamma(y') = \langle \mu(y)\mu(y-y') \rangle$ of the depth variations of figure 3 along the two meridians of longitude (*a*) 145° W and (*b*) 127° W as a function of y' = lag (in degrees of latitude).

vorticity, would need to be modified if it were to include the effect of depth changes occurring within distances of kilometres or less. This is because there will be an additional adjustment in the flow near the bottom to conform to the topography which will then make possible wave motions which differ somewhat from those strictly controlled by potential vorticity. A complete understanding of the modification of planetary waves by a rough bottom would necessarily include such an effect. None the less, the analysis presented here is as accurate as the data will allow and does give a first insight into the influence of the rough terrain on planetary-wave propagation, demonstrating that such influence is far from negligible.

Besides the absence of information at scales less than 15′ of latitude in the autocovariances, there is also an absence of large-scale information because of the finite length of the record. As with any other data set obtained from a physical process, our results are based on a denumerable collection of discrete values. Hence the number of samples within the population on which the autocovariances are based decreases with increasing lag. It can be considered, in effect, that values of these functions for lags greater than 10–20 % of the total number of data points do not give a true representation of the mean variance of the process. At large lags, therefore, it is not really valid to talk of an ensemble average since the averaging process involves so few realizations of the particular wavelength.

For this reason, the autocovariances in figure 4 have been arbitrarily truncated at a lag corresponding approximately to the limit at which all data points can be used in the calculations. Within this cut-off, however, the figures do show that besides the topographic microstructure there do exist more regular variations having scales of about 6° of latitude ($\sim 600\,\mathrm{km}$) resulting from the spacing of the larger fracture zones. In a more rigorous treatment, both these variations, which are essentially part of the deterministic problem, and the trend would have to be removed from the autocovariances. However, as the amplitude of these variations remains relatively small, we shall assume that the mean depth in the direction across the fractures is uniform, and concentrate our attention on the small-lag region of the curves.

Using the calculated values of $\epsilon^2\Gamma(0)$, we may now determine numerically the phase speeds of the two planetary-wave components. Since the autocovariances indicate a short correlation length for the topography relative to typical planetary-wave scales, our numerical results will be applied to the short-correlation limit (3.7).

As indicated by the graphs of the depth autocovariance, we may take $\epsilon^2\Gamma(0) \simeq 2\times 10^{-3}$ as a typical value between 5° N and 50° N for the region under consideration, while representative values of the mean slope parameter for the same region are

$$m \simeq 0, \quad n \simeq 2\times 10^{-9}\,\mathrm{cm}^{-1}. \tag{3.8}$$

The remaining parameters are representative for 30° N:

$$f_0 \simeq 7\times 10^{-5}\,\mathrm{s}^{-1}, \quad \beta \simeq 2\times 10^{-13}\,\mathrm{cm}^{-1}\,\mathrm{s}^{-1}, \tag{3.9}$$

where also $\sigma < f_0$. Use of (3.8) and (3.9) in (2.19) shows that the requirement $\beta^* < 0$ is satisfied provided that θ is given approximately by

$$-35^\circ \leqslant \theta < 145^\circ. \tag{3.10}$$

Moreover, the assumption that the surface divergence effect is small ($\gamma_0 < \frac{1}{2}\beta^*/\sigma$) is reasonably valid if $\sigma < \frac{1}{2}f_0$ ($h_0 \simeq 5000\,\mathrm{m}$), although such a requirement is not essential to obtain physically meaningful results. Finally, the validity of the first-order smoothing is seen from (3.7) to necessitate

$$\epsilon^2\Gamma(0)\,(f_0\sigma^{-1}\sin\theta)^2 < 1, \tag{3.11}$$

which, for the particular oceanic region considered here, limits the wave frequency σ to the fairly restrictive range

$$10^{-1}\,|\sin\theta| < 2\sigma/f_0 < 1. \tag{3.12}$$

Since $\alpha = |\frac{1}{2}\pi|$ for the east–west orientated fracture zones in this part of the Pacific and θ is given by (3.10), the relation (3.11) is most restrictive for waves of a given scale propagating westward and least restrictive for those propagating northward. For planetary waves whose phase moves at an angle of 45° to the roughness contours, representing neither the most nor least restrictive direction, the range of wavelengths to which (3.12) corresponds is

$$600\,\mathrm{km} < \lambda < 10\,000\,\mathrm{km}.$$

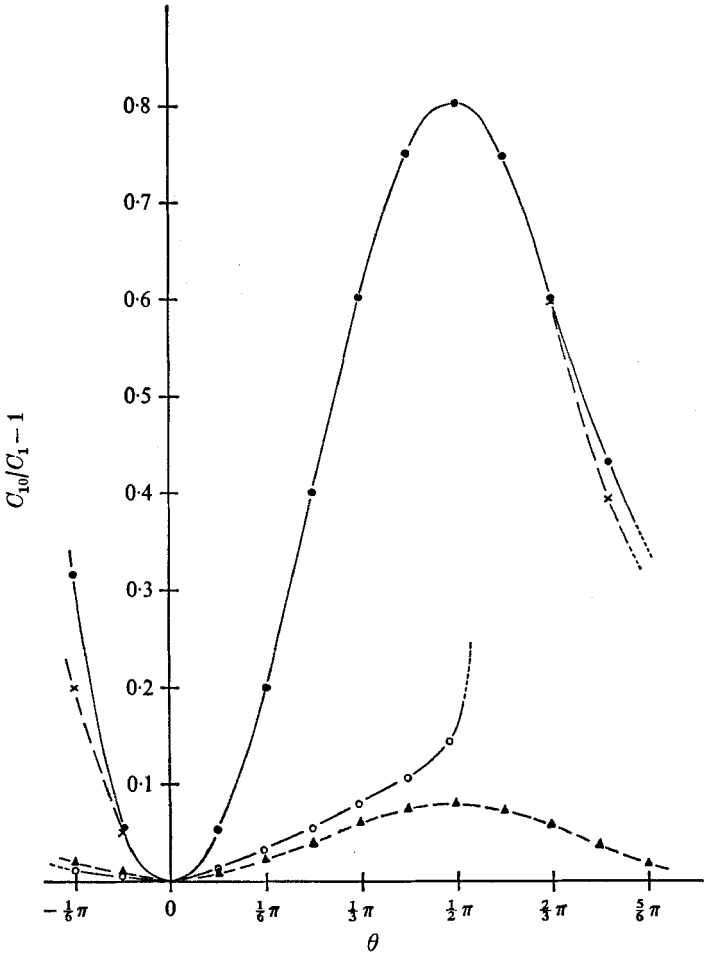

FIGURE 5. The phase speed C_1 of the short planetary-wave component as a function of the direction of propagation θ in the limiting cases $f_0/\sigma = 2$, 20 ($f_0 = 7 \times 10^{-5}\,\mathrm{s}^{-1}$). Divergent surface motions: —○—, $f_0/\sigma = 2$; —●—, $f_0/\sigma = 20$. Non-divergent surface motions ($\gamma_0 = 0$): – – ▲ – –, $f_0/\sigma = 2$; – – × – –, $f_0/\sigma = 20$. The angle θ is measured counterclockwise from north since the random components of topography are aligned east–west. C_{10} is the zeroth-order phase speed in the absence of random depth variations.

This is reasonably acceptable considering that the roughness has scales of order just under 100 km, and that the upper limit is anyway determined by the requirement that f should change little over a wavelength. For the values (3.9), the latter limits the longitudinal projection of wavelengths to scales less than 20 000 km.

Figure 5 is a plot of the relative phase speed for the short wave component in the limiting cases $\sigma = \frac{1}{2}f_0$ and $\sigma = \frac{1}{20}f_0$. As a comparison, we have also included corresponding curves for the rigid-lid case (vanishing surface divergence). In each example, the curves show zero phase speed when fluid motions are parallel to the strike of the fracture zones. Except for the surface divergent case ($\sigma = \frac{1}{2}f_0$), maximum phase-speed changes occur when the fluid motions are at right angles

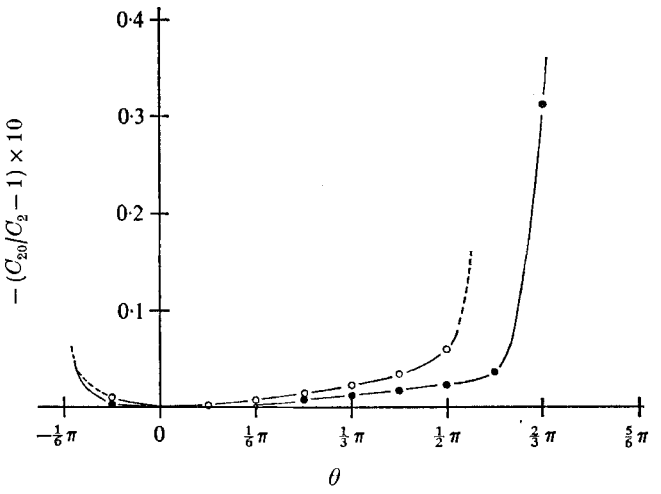

FIGURE 6. The phase speed C_2 of the long planetary-wave component as a function of the direction of propagation θ in the limiting cases $f_0/\sigma = 2$, 20 ($f_0 = 7 \times 10^{-5}\,\mathrm{s}^{-1}$) for divergent surface motions only: —○—, $f_0/\sigma = 2$; —●—, $f_0/\sigma = 20$. The angle θ is measured counter-clockwise from north. C_{20} is the phase speed in the absence of random depth variations.

to the fractures. The exception in this case arises because for $\sigma = \frac{1}{2}f_0$ the approximation $\gamma_0 < \frac{1}{2}\beta^*/\sigma$ used in the derivation fails for angles θ greater than 90°. It is also apparent from this figure that the relative difference in phase speed decreases as the frequency of the waves increases (longer waves) for a given direction of propagation.

The speed difference for the long planetary-wave component is plotted in figure 6. In contrast to the short-component case, the relative change increases as the frequency is increased. Moreover, there is not an angle of maximum change within the limits of the approximations which are valid for $\theta > \frac{1}{2}\pi$. Again, there is no difference in the phase speeds for waves propagating over a rough topographic region and for those propagating over a smoothly varying region when the fluid motions are parallel to the strike of the roughness elements. Finally, in the absence of any surface divergence K_{20} vanishes, leaving only the short wave component as a truly propagating wave.

4. Discussion and summary

In the previous sections we have described certain properties of planetary waves travelling over a rough bottom whose scale heights are much less than the total fluid depth. Since the topography in the present problem is a one-dimensional random variable, however, we are able to derive only the statistical values of the properties involved, whereby the wavenumber magnitude for a particular direction of propagation has small correction terms involving mean-square terms and transform functions for the topography. As with most problems of this nature, the mean-square terms measure the accumulated effect of the randomly situated 'scatterers' on the wave motion. The transform terms, on the other

hand, measure the integrated effect between the scales of the propagating waves and those related to the spacing of the scatterers.

From the inviscid equations in § 2, it is possible to show that the potential vorticity Π associated with a fluid column must be conserved during its motion; viz.,

$$D\Pi/Dt = 0, \tag{4.1}$$

where

$$\Pi = (f+\zeta)/h, \tag{4.2}$$

$D/Dt = \partial/\partial t + \mathbf{u}.\nabla$ is the Lagrangian derivative and $\zeta = (\nabla \times \mathbf{u})_z$ is the vertical component of relative vorticity. For any fluid column, a readjustment in its absolute vorticity $f+\zeta$ is required if the length h of its vortex lines is altered during its motion. Thus changes in depth are analogous to a restoring mechanism for planetary-wave motions, which, in the case of the short wave component for fixed frequency, produces a decrease (increase) in the wavenumber magnitude for a decrease (increase) in the restoring force. In our model, that part of the topographic restoring mechanism ($\sim f\nabla h$) which is associated with changes in the mean depth appears only in the deterministic part of the solution through the parameters m and n, and essentially generates a wavenumber whose phase moves with deep water to its left (right) in the northern (southern) hemisphere. When considered with the wavenumber generated by the β-effect, this results in a change in the possible directions of phase propagation.

The integrated contribution to the topographic restoring mechanism associated with the random depth component is determined by (2.25), the real part of this expression measuring the effective change in phase speed brought about by the random forcing while the imaginary part takes into account the backscattering tendency of the rough topography as it inhibits the passage of the fluid. By itself, the larger of the two real terms in (2.25), $\Gamma(0)$, is a measure of the mean-square increase in the effective restoring force brought about by the increased distance of travel of a fluid column that is conserving potential vorticity. The smaller term, expressed via the sine transform, is slightly more difficult to account for. Letting $A_j^2 = [(f_0/\sigma)\, K_{j0} \sin\theta]^2$ we find

$$A_j^2\, 2(k_{j0}-B) \int_0^\infty \Gamma(\hat{\xi}) \sin[2(k_{j0}-B)\,\hat{\xi}]\, d\hat{\xi} = A_j^2\, 2(k_{j0}-B)\, \phi_j |2(k_{j0}-B)|, \tag{4.3}$$

where ϕ_j is the 'quad-spectrum' at the wavenumber $2(k_{j0}-B)$. Since it can be shown that the ξ component of the group velocity is to $O(\epsilon^2)$

$$C_{gk} = -2(k_{j0}-B)\, \sigma/(k_{j0}^2 + l_{j0}^2 + \gamma_0^2),$$

the wavenumber $2(k_{j0}-B)$ is proportional to the amount of energy flux across the contours associated with the random depth variations, and is therefore a scale for the spatial modulation of the wave amplitude in that direction. The even function $A_j^2\, 2(k_{j0}-B)\, \phi_j$ is then a measure of the effective mean-square fractional height which results from an out-of-phase (90°, 270°, ...) interaction between the depth-induced variations in the wave and the spatially modulated wave amplitude. In other words, the transform integral takes into account the integrated effect of differences in the depth-induced relative vorticity between adjacent fluid columns as a result of their differences in path length, the latter being a

consequence of the spatial modulation of wave amplitude. If there is any consistency in the variation of this difference along a wave front, as a result of any periodic component in the depth variations whose scale is near to that of the spatially modulated amplitude, a net relative vorticity field will exist. This will act as an effective restoring force on the wave. Clearly, if the depth changes are only weakly correlated and/or the argument of ϕ_j is small, the term (4.3) will be small compared with the $\Gamma(0)$ term, as in the case of the short-correlation limit of § 3. The effect vanishes if there is no distortion of the fluid paths by the random depth variations ($A_j^2 = 0$) or if there is no component of amplitude modulation across the contours ($k_{j0} - B = 0$).

The cosine transform term in (2.25), which gives the decrease in wave amplitude in the direction of energy propagation, can be written in an analogous manner to (4.3); viz.

$$A_j^2 2|k_{j0} - B| \int_0^\infty \Gamma(\xi) \cos[2(k_{j0} - B)\xi] d\xi = A_j^2 2|k_{j0} - B| \, \phi_j^*[2(k_{j0} - B)],$$

where ϕ_j^* is now the 'co-spectrum'. In this sense, it is a measure of the effective height of the scatterers resulting from the in-phase interaction of the amplitude-modulated wave with the distorted wave paths. The more closely the spatial scales correspond, in this case, the more effectively the topography is behaving as an energy backscatterer. In the limit of short correlation lengths (cf. § 3), the spatial coherence of any scattered energy is so small that it produces negligible energy loss.

Since the short-correlation limit will pertain in most physically realizable situations, we may summarize our results as follows. First, the effect of the bottom roughness is to increase (decrease) the wavenumber magnitude of the shorter (longer) wave component from that for a smoothly varying topography for waves of constant frequency. As a result, the phase speed and group-velocity magnitude of the shorter (longer) waves are decreased (increased). The only exception is if the actual fluid motions are parallel to roughness contours, when no relative speed change occurs. Second, numerical values obtained from hydrographic charts of the western North Pacific indicate that the phase speed of the shorter component may be significantly altered by roughness features in the real ocean. Finally, both wave components lose energy in the direction of energy propagation because of backscattering. These results are in basic agreement with the findings of Rhines & Bretherton, who used a deterministic approach to the same general problem.

The assistance of Liliane Kuwahara in obtaining the numerical values used in this paper is gratefully acknowledged. Also, my sincerest thanks to Dr J. Huthnance for pointing out an important error in the original manuscript and to Prof. R. W. Stewart and Prof. M. S. Longuet-Higgins for their critical review of the work.

REFERENCES

BUCHWALD, V. T. 1972 Energy and energy flux in planetary waves. *Proc. Roy. Soc.* A **328**, 37–48.

CHASE, T. E., MENARD, H. W. & MAMMERICKX, J. 1970 Bathymetry of the North Pacific. *Scripps Inst. Oceanog. & Inst. Mar. Res., University of California, Rep.*

KELLER, J. B. 1967 The velocity and attenuation of waves in random medium. In *Electromagnetic Scattering* (ed. R. L. Rowell & R. S. Stein), pp. 823–834. Gordon & Breach.

KELLER, J. B. & VERONIS, G. 1969 Rossby waves in the presence of random currents. *J. Geophys. Res.* **74**, 1941–1951.

LONGUET-HIGGINS, M. S. 1964 Planetary waves on a rotating sphere. *Proc. Roy. Soc.* A **279**, 446–473.

LONGUET-HIGGINS, M. S. 1965 Planetary waves on a rotating sphere, II. *Proc. Roy. Soc.* A **284**, 40–54.

RHINES, P. B. 1969*a* Slow oscillations in an ocean of varying depth. Part 1. Abrupt topography. *J. Fluid Mech.* **37**, 161–189.

RHINES, P. B. 1969*b* Slow oscillations in an ocean of varying depth. Part 2. Islands and seamounts. *J. Fluid Mech.* **37**, 191–205.

RHINES, P. B. 1970 Wave propagation in a periodic medium with application to the ocean. *Rev. Geophys.* **8**, 303–319.

RHINES, P. B. & BRETHERTON, F. 1973 Topographic Rossby waves in a rough-bottomed ocean. *J. Fluid Mech.* **61**, 583–607.

ROSSBY, C. G. 1939 Relation between variations in the intensity of the zonal circulation of the atmosphere and the displacements of the semi-permanent centres of action. *J. Mar. Res.* **2**, 38–55.

THOMSON, R. E. 1973 Energy and energy flux in planetary waves in a variable depth ocean. *Geophys. Fluid Dyn.* **5**, 385–399.

VERONIS, G. 1966 Rossby waves with bottom topography. *J. Mar. Res.* **24**, 338–349.